Metallurgical and Materials Data (2026): x-x

Publisher: Association of Metallurgical Engineers of Serbia

Metallurgical and Materials Data

www.metall-mater-data.com

First-principles investigation of the structural, elastic, and electronic properties of half-Heusler compounds LiTiB and LiTiAl

Radja Nour El Imene Bennoui*

University of Science and Technology of Oran Mohamed Boudiaf (USTO-MB), Faculty of Physics, Department of Engineering Physics, Laboratory of Analysis and Application of Radiations (LAAR), 1505 El Menouar 31000, Oran, Algeria.

ARTICLE INFORMATION:

https://doi.org/10.56801/MMD75

Received: 23 October 2025
Accepted: 23 January 2026

Type of paper: Research paper

ABSTRACT

This study presents a first-principles investigation based on density functional theory (GGA) of the Half-Heusler compounds LiTiB and LiTiAl. Structural stability was evaluated through total energy optimization of three possible atomic configurations, with the Type-II phase identified as the energetically most favorable. Mechanical stability is confirmed by the calculated elastic constants, which satisfy the Born stability criteria. The derived mechanical parameters indicate that LiTiAl exhibits greater ductility, whereas LiTiB demonstrates higher stiffness. Both compounds exhibit metallic behavior, as evidenced by their electronic band structures and density of states. The electronic states near the Fermi level are predominantly governed by Ti d-states, while contributions from B p- or Al p-states are minor, and Li shows negligible participation. These findings indicate that LiTiB and LiTiAl are structurally stable and mechanically robust Half-Heusler metallic alloys with potential relevance for structural and functional applications.

Keywords: Half-Heusler compounds, LiTiB, LiTiAl, Density Functional Theory, Elastic properties, Electronic properties.

1. Introduction

Half-Heusler (HH) compounds form a well-established family of ternary intermetallic materials that have drawn sustained interest over the past decades. This attention stems from their simple cubic C1b crystal structure (space group $F\bar{4}3m$) combined with an exceptional diversity of physical properties. Depending on their chemical composition, HH compounds can exhibit semiconducting, metallic, half-metallic, or even topological electronic behavior, which makes them attractive for a broad range of applications, including thermoelectric, spintronics, and energy-related technologies (Graf et al. 2011, Felser at al. 2007, Chadov et al. 2010).

From a theoretical standpoint, density functional theory (DFT) has emerged as a reliable and widely used framework for exploring the fundamental properties of HH materials. First-principles calculations have been successfully applied to predict structural stability, elastic behavior, and electronic characteristics, often providing guidance for experimental synthesis and materials design (Hohenberg and Kohn 1964, Kohn and Sham 1965, Sinh and Nordström 2006). Importantly, it has become increasingly clear that the functional performance of HH compounds cannot be assessed solely on the basis of their electronic structure. Mechanical stability and elastic response play a critical role in determining the feasibility of material processing, device integration, and long-term operational reliability (Mouhat and Coudert 2014, Hill 1952, Pugh 1954). Therefore, a combined analysis of structural, elastic, and electronic properties is essential for a realistic and meaningful evaluation of HH compounds.

Within this materials class, Ti-based half-Heusler compounds occupy a particularly important position. The presence of Ti introduces partially filled 3d states, which strongly influence the electronic structure and transport behavior. Several Ti-containing HH systems, such as TiNiSn and TiCoSb, have been extensively investigated and shown to possess favorable electronic properties for functional applications (Tobola and Pierre 2000, Al Rahal Al Orabi et al. 2017, Wang et al. 2020). In contrast, Li-based Ti-half-Heusler compounds have received considerably less attention, especially with regard to their elastic and mechanical properties. Moreover, existing studies tend to focus on a limited number of compositions, leaving open questions about how different p-block elements affect bonding characteristics, elastic stiffness, and electronic behavior in Li–Ti–Z (Z = p-element) systems.

In this respect, LiTiB and LiTiAl represent two particularly appealing yet largely unexplored candidates. Both compounds share the same crystallographic framework and transition-metal component, while differing only in the nature of the Z element (B versus Al). This makes them an ideal model system for examining how changes in p–d hybridization influence structural stability, elastic constants, and electronic properties. Replacing B with Al is expected to alter the bonding environment, charge distribution, and electronic dispersion near the Fermi level, which in turn may affect both mechanical stiffness and metallic character. Despite this clear scientific motivation, a systematic and comparative first-principles investigation of LiTiB and LiTiAl that simultaneously addresses their structural, elastic, and electronic properties is still missing from the literature.

* Corresponding author
E-mail address: radjanourelimene.bennoui@univ-usto.dz (Radja Nour El Imene Bennoui)

Motivated by this gap, the present work presents a comprehensive ab initio study of LiTiB and LiTiAl within the framework of DFT using the generalized gradient approximation. Equilibrium structural parameters and relative phase stability are first examined, followed by a detailed evaluation of the elastic constants to assess mechanical stability and resistance to deformation. The derived mechanical moduli provide further insight into bonding characteristics and ductility. In addition, the electronic band structures and densities of states are analyzed to clarify the origin of the metallic behavior and the role of orbital contributions near the Fermi level. By integrating these results, this study aims to establish clear structure–property relationships for LiTiB and LiTiAl and to provide reliable reference data for future theoretical and experimental investigations of Li-based half-Heusler compounds.

2. Computational details

First-principles calculations were carried out within the framework of density functional theory (DFT) using the full-potential linearized augmented plane wave (FP-LAPW) method as implemented in the WIEN2k package (Blaha et al. 2020, Blaha et al. 2001). The exchange–correlation potential was treated using the generalized gradient approximation (GGA) in the Perdew–Burke–Ernzerhof (PBE) parametrization (Perdew 1996).

The all-electron full-potential linearized augmented plane wave (FP-LAPW) method, as implemented in the WIEN2k code, is among the most accurate techniques within density functional theory for total-energy and elastic-property calculations. Its full-potential and all-electron treatment is particularly well suited for cubic intermetallic systems, ensuring reliable stress–strain relations and precise determination of elastic constants.

Both LiTiB and LiTiAl crystallize in the cubic C1b half-Heusler structure (Figure 1) with space group *F*-43*m* (No. 216). Three possible atomic configurations (Type I, Type II, and Type III) were considered, corresponding to different occupations of the Wyckoff positions 4a, 4b, and 4c, as summarized in Table 1 (de Groot et al. 1983). For each configuration, the equilibrium structural parameters were determined by fitting the total energy as a function of volume to the third-order Birch–Murnaghan equation of state. The most stable configuration was identified by comparing the total energies of the optimized structures.

The muffin-tin radii (RMT) were chosen to ensure an accurate description of the wave functions while avoiding sphere overlap. The plane-wave cutoff was controlled by setting RKmax=9. Brillouin-zone integrations were performed using a 9×9×9 Monkhorst–Pack k-point mesh (Methfessel and Paxton 1989), which was found sufficient to ensure convergence of the total energy. Self-consistent calculations were considered converged when the total energy difference between successive iterations was less than 10–5 Ry. The valence electronic configurations used in the calculations were Li: [He] 2s1, Ti: [Ar] 3d24s2, B: [He] 2s22p1, and Al: [Ne] 3s23p1.

The elastic constants C11, C12, and C44 were evaluated using the finite-strain method by applying small symmetry-conserving deformations to the optimized cubic structures. Strain amplitudes of δ=±0.005 and ±0.01 were employed. For each strained configuration, the total energy was recalculated and fitted to a second-order polynomial. Internal atomic positions were fully relaxed to obtain accurate elastic responses. The macroscopic mechanical properties, including the bulk modulus B, shear modulus G, Young's modulus E, and Poisson's ratio v, were derived using the Voigt–Reuss–Hill averaging scheme (Mouhat and Coudert 2014).

The electronic band structures were calculated along the high-symmetry directions of the cubic Brillouin zone (W–L–Γ–X–W–K). The total and partial densities of states (DOS and PDOS) were computed using a denser k-point mesh to ensure smooth spectra. All electronic energies were referenced to the Fermi level, which was set to 0 eV (Marder 2010).

Table 1. Three possible atomic configurations

Type	4a (X)	4b (Y)	4c (Z)
Type I	(1/4,1/4,1/4)	(0,0,0)	(1/2,1/2,1/2)
Type II	(0,0,0)	(1/2,1/2,1/2)	(1/4, 1/4,1/4)
Type III	(1/2,1/2,1/2)	(¼,1/4,1/4)	(0,0,0)

3. Results and discussion

3.1. Structural properties

The structural properties and relative stability of LiTiB and LiTiAl were investigated by optimizing the total energy as a function of the unit-cell volume within the GGA-PBE approximation. Both compounds crystallize in the cubic C1b half-Heusler structure, for which three possible atomic configurations (Type I, Type II, and Type III) were considered. For each configuration, total-energy calculations were performed and fitted using the third-order Birch–Murnaghan equation

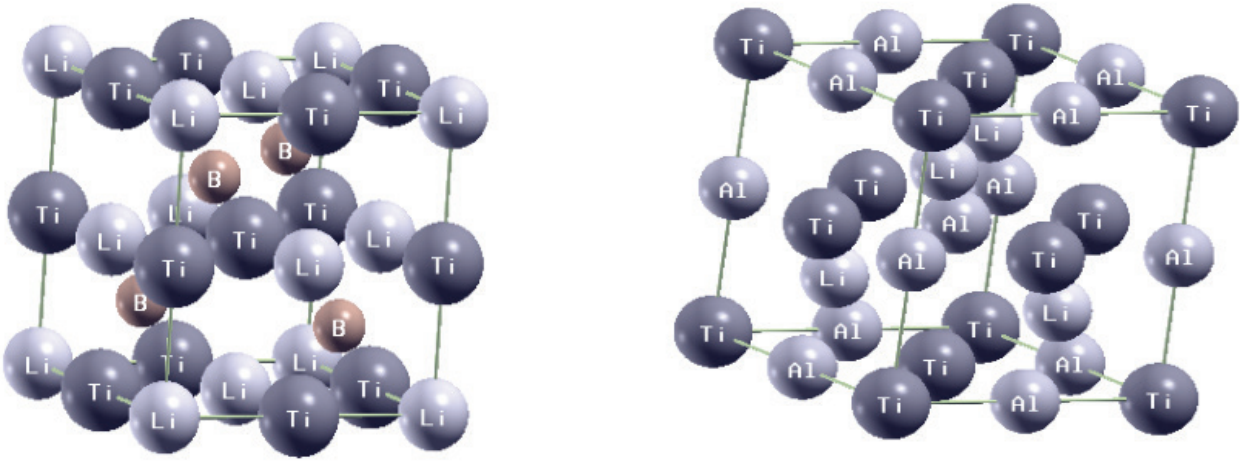

a) b)

Fig. 1. Crystal structure of: a) LiTiB and b) LiTiAl half-Heusler compound

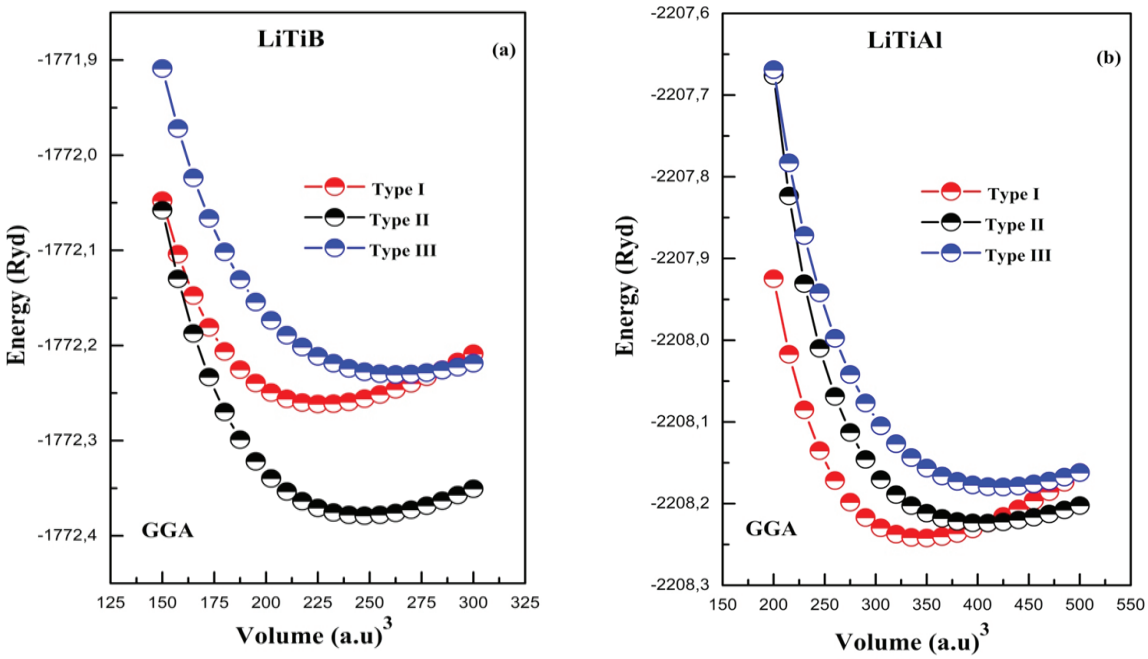

a) b)

Fig. 2. Total energy as a function of unit cell volume for the compounds studied: a) LiTiB and b) LiTiAl.

of state to determine the equilibrium lattice parameters and assess the energetic stability.

The calculated energy–volume curves for LiTiB and LiTiAl are presented in Figure 2(a) and Figure 2(b), respectively. For LiTiB, the Type II configuration exhibits the lowest total energy among the three considered arrangements, indicating that it is the most stable ground-state structure. In contrast, LiTiAl is found to favor the Type I configuration, which lies energetically below the corresponding Type II and Type III configurations. These results clearly demonstrate that the structural stability of Li-based half-Heusler compounds is strongly dependent on the atomic arrangement and the chemical nature of the Z element. To further quantify this stability hierarchy, the relative energy differences (ΔE) between the competing configurations are calculated and discussed in detail below.

Relative Energy Differences and Ground-State Stability

Table 2 summarizes the optimized structural parameters obtained from fitting the total energy–volume data to the Murnaghan state equation (Murnaghan 1944), as well as the associated equilibrium volumes and Bulk modules.

$$E(V) = E_0 + \frac{B_0 V}{B_0'}\left[\frac{\left(\frac{V_0}{V}\right)}{B_0'} + 1\right] - \frac{B_0 V_0}{B_0' - 1} \quad (3.1)$$

E(V) = total energy at volume V
E_o = minimum energy at equilibrium volume V_o
B_o = Bulk modulus
B_o' = derivative Bulk modulus

Table 2. Structural parameters and relative total energies of LiTiB and LiTiAl for different atomic configurations

Compound	configuration	Lattice constant a (A°)	V_o (a.u.³)	B (GPa)	B′	E_o (Ry)	ΔE (meV/f.u.)
LiTiB	Type I	5.127	227.33	108.3	4.20	−1772.26166	1595
	Type II	5.272	247.21	**103.0**	**3.93**	−1772.37894	0
	Type III	5.381	262.81	82.1	3.55	−1772.23051	2019
LiTiAl	Type I	5.898	346.13	61.2	3.86	−2208.24219	0
	Type II	6.209	403.73	46.1	3.82	−2208.22865	184
	Type III	6.286	418.97	44.0	3.57	−2208.17928	856
LiTiAl	Other study (Zhang et al. 2025)	6.191					

*Note: Energy conversion: 1Ry = 13.605693 eV = 13605.693 meV.

For each compound, the relative energy difference ΔE between a given atomic configuration and the most stable (ground-state) configuration was calculated using:

$$\Delta E = E_{Type} - E_{ground} \quad (3.2)$$

Where E ground is the lowest total energy among the considered configurations.

The total energies are reported in Rydberg (Ry), while the relative energy differences (ΔE) between the different atomic configurations are expressed in meV per formula unit (meV/f.u.)

A quantitative comparison of the total energies for the three atomic configurations reveals distinct ground-state preferences for LiTiB and LiTiAl. For LiTiB, the Type II configuration is energetically favored, lying lower in energy than the Type I and Type III configurations 1595 meV and 2019 meV per formula unit, respectively. This ground-state structure is associated with an equilibrium lattice constant of 5.272 Å, which lies between the smaller lattice parameter of Type I (5.127 Å) and the larger value obtained for Type III (5.381 Å). In contrast, LiTiAl stabilizes in the Type I configuration, characterized by an equilibrium lattice constant of 5.898 Å, while the Type II and Type III configurations exhibit larger lattice parameters of 6.209 Å and 6.286 Å and are higher in energy by about 184 meV and 856 meV per formula unit, respectively. This energetic preference for more compact structures is consistent with the calculated bulk modulus values, as the ground-state configurations in both compounds exhibit higher resistance to volume compression compared to their less stable counterparts. These results highlight the strong interplay between atomic arrangement, lattice expansion, and mechanical stiffness in Li-based half-Heusler compounds.

3.2. Elastic properties

The elastic constants of the half-Heusler compounds were obtained (Table 3) using the standard energy–strain method. Small volume-conserving deformations were applied to the relaxed cubic cell, and the total energy E(δ) was calculated for a series of strain amplitudes δ. The final strain set was:

δ=0, ±0.0025, ±0.005, ±0.0075, ±0.01.

We also verified that the reduced set {0, ±0.005, ±0.01} yields consistent results.

For each strained configuration, internal atomic coordinates were relaxed (relaxed-ion calculations) until the forces were below 10^{-3} Ry/bohr, with an SCF energy convergence threshold of 10^{-5} Ry.

In order to evaluate the mechanical behavior and stability of crystalline materials, elastic constants are crucial. The three independent elastic constants for a cube system are C11, C12 and C44. Table 3 displays the determined values for LiTiB and LiTiAl. In accordance with the Born stability conditions for cubic crystals, which are C11-C12 > 0, C11+2C12 > 0 and C44 > 0, tetragonal and rhombohedral distortions are applied to the cubic structure while maintaining equilibrium volume in order to calculate these elastic constants (Mogulkoc and Ciftci 2017).

Both LiTiB and LiTiAl satisfy the Born stability criteria for cubic systems, confirming their mechanical stability at equilibrium.

To evaluate the macroscopic mechanical properties, the Voigt–Reuss–Hill (VRH) averaging scheme was employed. The bulk modulus B, shear modulus G, Young's modulus E, Poisson's ratio v, and Pugh's ratio B/G were derived from the calculated elastic constants (Pugh 1954):

Bulkmodulus: B=(*C*11+2*C*12)/3 (3.3)

Shearmodulus (Voigt - Reuss - Hillaverage): G=(*C*11-*C*12+3*C*44)/5 (3.4)

Young' modulud: E=9 BG/3 B+G (3.5)

Pugh' sratio: *B*/*G* (3.6)

Poisson' sratio: v=3*B*-2*G*/2 (3B+G) (3.7)

The results (Table 4) indicate that LiTiB exhibits a significantly higher bulk modulus (100.15 GPa) and shear modulus (63.05 GPa) compared to LiTiAl (58.08 GPa and 25.83 GPa, respectively), reflecting its greater resistance to volume compression and shear deformation. Consistently, LiTiB also shows a higher Young's modulus (156.3 GPa), indicating superior stiffness relative to LiTiAl (67.4 GPa).

The Poisson's ratio values further support these observations. LiTiB exhibits a lower value (v=0.24), suggesting a relatively more directional and covalent bonding character, whereas LiTiAl shows a higher value (v=0.31), indicative of increased metallic bonding contributions. According to Pugh's criterion, materials with B/G<1.75 are expected to be brittle, while those with B/G>1.75 tend to be ductile. Based on this criterion, LiTiB (B/G=1.59) can be classified as brittle, whereas LiTiAl (B/G=2.25) exhibits a ductile mechanical behavior. These differences highlight the strong influence of the Z-element substitution on the mechanical response of Li-based half-Heusler compounds.

Table 3. Elastic constants (GPa) of LiTiB and LiTiAl

Compound	C_{11} (GPa)	C_{12} (GPa)	C_{44} (GPa)
LiTiB	221.21	39.62	49.23
LiTiAl	81.65	46.29	33.32
Study for LiTiAl (Mogulkoc and Ciftci 2017)	63.26	41.59	22.85

Table 4. Derived mechanical properties of LiTiB and LiTiAl

Compound	B (GPa)	G (GPa)	E (GPa)	B/G	v
LiTiB	100.15	63.05	156.3	1.59	0.24
LiTiAl	58.08	25.83	67.4	2.25	0.31

For comparison, the elastic constants of LiTiAl reported in a previous study were also analyzed using the same Voigt–Reuss–Hill averaging scheme. Using the reported values C11=63.26 GPa, C12=41.59 GPa, and C44=22.85 GPa, the corresponding bulk, shear, and Young's moduli were found to be 48.81 GPa, 18.55 GPa, and 49.2 GPa, respectively. Although these values are lower than those obtained in the present work, both studies consistently indicate a relatively soft and ductile mechanical character for LiTiAl. The higher Poisson's ratio (≈0.33) and larger Pugh's ratio (B/G>2) in both cases confirm the dominance of metallic bonding and the ductile nature of LiTiAl. The quantitative differences can be attributed to variations in computational parameters, equilibrium lattice constants, and exchange–correlation treatments.

3.3. Electronic properties

3.3.1 The electronic density of states (DOS) of LiTiB and LiTiAl

A comparative analysis of the electronic density of states (DOS) of LiTiB and LiTiAl reveals that both compounds exhibit metallic character (Figure 3 and 4), as evidenced by the finite total DOS at the Fermi level (set to 0 eV). In both systems, the electronic states in the immediate vicinity of the Fermi energy (approximately −1 to +1 eV) are dominated by Ti-3d orbitals, while the contributions from Li atoms are negligible, indicating that electronic transport is primarily governed by Ti-derived d states.

Despite these similarities, notable differences arise in the valence-band region due to the different p-block elements. For LiTiB (Figure 3), the valence band extends from approximately −7 eV to the Fermi level and is characterized by strong hybridization between Ti-3d and B-2p states, with B-2p contributions mainly distributed in the deeper energy range between −6 and −3 eV. This pronounced hybridization reflects relatively strong covalent Ti–B interactions. In contrast, LiTiAl (Figure

4) exhibits a valence band extending from about −6 eV to 0 eV, where Al-3p states contribute primarily between −5 and −2 eV, overlapping with Ti-3d states and indicating comparatively weaker Ti–Al hybridization.

In the conduction-band region (E > 0 eV), both compounds show DOS profiles dominated by Ti-3d states, extending up to approximately +6 eV, with several peaks associated with the crystal-field splitting of the Ti-d manifold. However, the overall DOS intensity near the Fermi level is higher for LiTiAl than for LiTiB, suggesting enhanced metallic character in LiTiAl.

Overall, the comparative DOS analysis demonstrates that while both LiTiB and LiTiAl are Ti-dominated metallic half-Heusler compounds, substitution of B by Al significantly modifies the p–d hybridization and the distribution of valence states. The stronger Ti–B covalent interaction in LiTiB correlates with its relatively enhanced bonding strength, whereas the higher DOS at the Fermi level in LiTiAl indicates increased electronic delocalization, which may influence transport properties.

The orbital-resolved DOS shown in Figure 5 allows a qualitative visualization of the relative contributions of s, p, and d states across the energy range.

3.3.2 Electronic band structure

For LiTiB:

The electronic band structure of LiTiB calculated along the high-symmetry directions W–L–Γ–X–Z–W–K is shown on the left of Figure 6. The results indicate a metallic character, as several electronic bands cross the Fermi level E_F without the opening of a direct or indirect energy gap. Quantitatively, at least two dispersive bands intersect the Fermi level along the Γ–X and X–Z directions. These bands exhibit energy dispersion of approximately 1.5–2.0 eV near the Γ point, suggesting relatively low effective masses for the charge carriers. The valence band region extends from about −6.5 eV up to E_F, while the conduction bands start immediately above the Fermi level and reach energies of approximately +7.5 eV. In addition, relatively flat bands are observed in the lower energy region below −5 eV, indicating localized electronic states, whereas the bands near the Fermi level are more dispersive and thus primarily responsible for the metallic conductivity of LiTiB.

For LiTiAl

On the right of Figure 6 the calculated band structure of LiTiAl along the same high-symmetry path is presented. Similar to LiTiB, LiTiAl exhibits metallic electronic structure, with no band gap observed at the Fermi level. Compared to LiTiB, a larger number of bands (three to four) cross the Fermi level in LiTiAl, particularly around the Γ and X points. The dispersion of these bands reaches approximately 2.0–2.5 eV, which is larger than that observed in LiTiB, indicating enhanced carrier mobility. The valence band region spans roughly from −6.0 eV to 0 eV, while the conduction bands extend up to about +8.0 eV, resulting in a slightly wider overall bandwidth. The increased number of Fermi-level crossings and stronger band dispersion in LiTiAl reflect

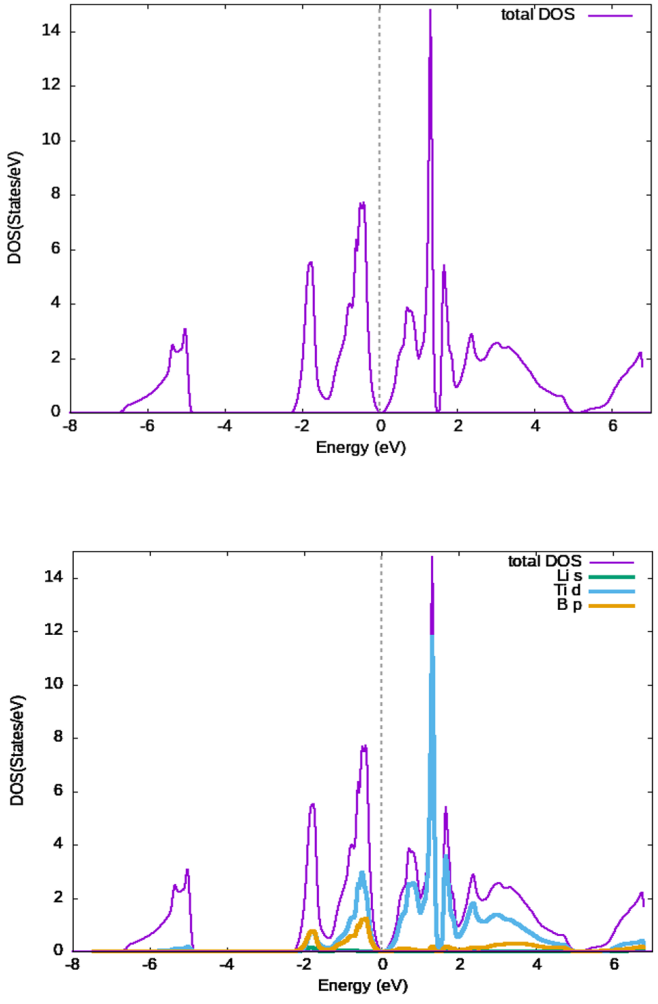

Fig. 3. TDOS and PDOS of LiTiB

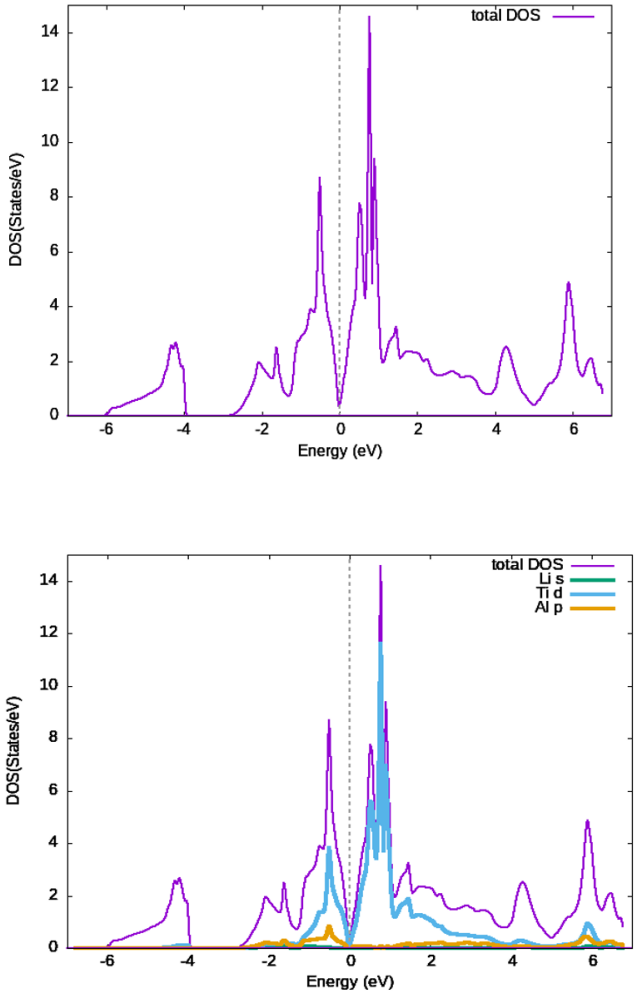

Fig. 4. TDOS and PDOS of LiTiAl

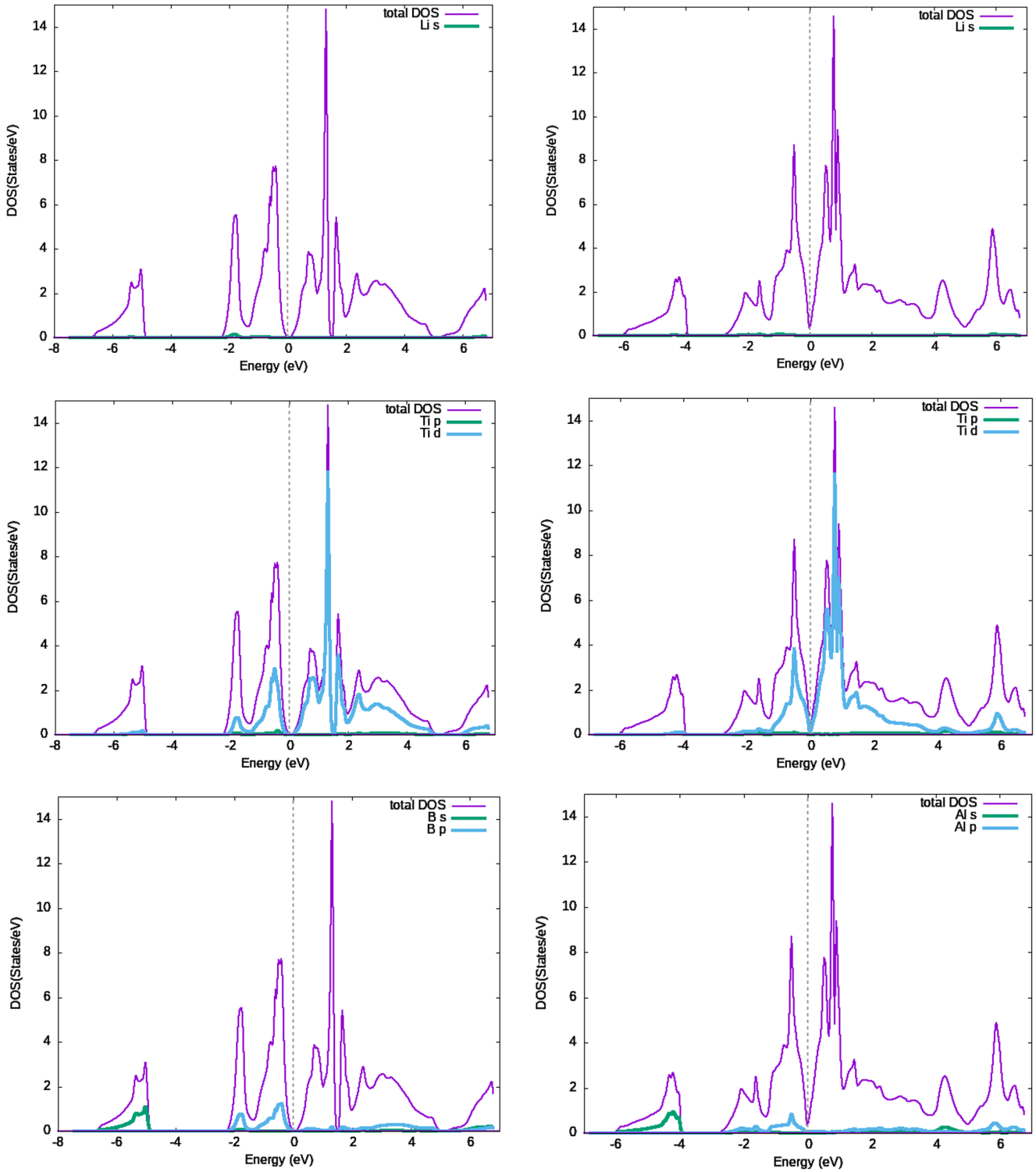

Fig. 5. Total density of states (TDOS) and partial density of states (PDOS) of LiTiZ (Z = B, Al), illustrating the contributions of the s, p, and d orbitals for each compound.

enhanced electronic interactions compared to LiTiB, leading to more pronounced metallic behavior.

3.3.3 Comparative Discussion with Other Half-Heusler Compounds

To place the present results in a broader context, a comparison with representative half-Heusler compounds reported in the literature is presented:

Although both LiTiB and LiTiAl exhibit metallic electronic structures characterized by multiple bands crossing the Fermi level, their behavior differs markedly from that of several well-known half-Heusler compounds reported in the literature. For instance, semiconducting half-Heusler alloys such as CoTiSb and NiTiSn display well-defined energy band gaps arising from their 18-valence-electron configurations (Lee at al. 2011). In contrast, LiTiB and LiTiAl deviate from this electron-count rule, resulting in metallic band structures with no gap at the Fermi energy.

Similarly, Li-based half-Heusler compounds such as LiMgP and LiMgAs have been theoretically predicted to exhibit direct semiconducting band gaps of approximately 1.3–1.5 eV (Nashia et al. 2025). This comparison highlights the **critical** role of the Z-element in shaping the electronic band structure, as replacing Mg with Ti and P/

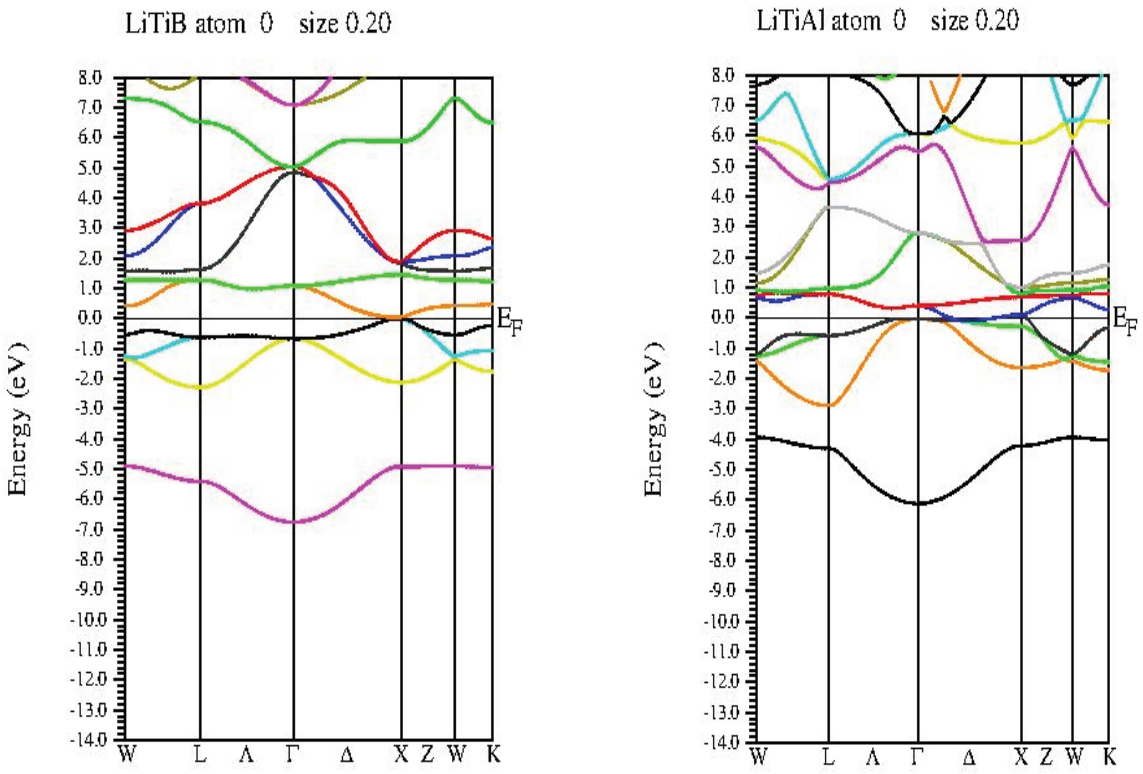

Fig. 6. Band structure of LiTiB and LiTiAl respectively.

As with B/Al leads to suppression of the band gap and the emergence of metallic behavior in LiTiB and LiTiAl.

In addition, half-metallic behavior has been reported in compounds such as NiMnSb, where one spin channel is metallic while the opposite channel exhibits a band gap, making these materials attractive for spintronic applications (Galanakis et al. 2002). Unlike these half-metallic systems, LiTiB and LiTiAl show metallic band crossings in both spin channels, further emphasizing the diversity of electronic properties within the half-Heusler family.

Overall, these comparisons demonstrate that while LiTiB and LiTiAl share a metallic character with several half-Heusler compounds, their electronic band structures are fundamentally different from semiconducting, topological, and half-metallic systems reported in previous studies, underscoring the strong dependence of electronic behavior on chemical composition and valence electron count.

3.3.4 Summary (DOS + Band Structure)

The combined analysis of the band structures and densities of states provides a consistent picture of the electronic behavior of LiTiB and LiTiAl. The multiple band crossings at the Fermi level observed in the band structures are fully supported by the finite DOS at EF, confirming the metallic nature of both compounds. In both systems, the states near the Fermi energy originate predominantly from Ti-3d orbitals, while Li contributions remain negligible, in agreement with the orbital-resolved DOS analysis. The differences in band dispersion and the number of Fermi-level crossings between LiTiB and LiTiAl are reflected in their respective DOS intensities at EF, indicating a higher metallic character for LiTiAl. Overall, the DOS and band-structure results are mutually consistent and demonstrate that the substitution of B by Al modifies the electronic dispersion and carrier density without altering the Ti-d–dominated metallic nature of the half-Heusler framework.

Conclusion

In this work, a comprehensive first-principles investigation of the half-Heusler compounds LiTiB and LiTiAl has been carried out in order to clarify their structural stability, elastic behavior, and electronic properties. By systematically examining the three possible atomic configurations (Type I, II, and III), the ground-state structures were unambiguously identified, revealing that LiTiB stabilizes in the Type II configuration, whereas LiTiAl favors the Type I arrangement. The calculated relative energy differences highlight the decisive role of atomic ordering in determining the structural stability of Li-based half-Heusler compounds.

The elastic constants and derived mechanical parameters were carefully recalculated using a corrected deformation protocol and the Voigt–Reuss–Hill averaging scheme, leading to physically reasonable values consistent with known trends in half-Heusler materials. The results indicate that both compounds satisfy the mechanical stability criteria for cubic crystals, while exhibiting moderate stiffness and distinct elastic responses. The observed differences in bulk modulus and elastic behavior between LiTiB and LiTiAl are directly linked to lattice expansion and the nature of chemical bonding associated with the substitution of B by Al.

Electronic structure calculations based on band structures and densities of states consistently show that both LiTiB and LiTiAl are metallic, with several bands crossing the Fermi level. In both systems, the electronic states near the Fermi energy are dominated by Ti-3d orbitals, while the Z-element mainly influences band dispersion and the density of states at the Fermi level. A comparative analysis reveals that LiTiAl exhibits a higher density of states at the Fermi level and stronger band dispersion than LiTiB, indicating a more pronounced metallic character.

Nevertheless, this work provides reliable and internally consistent reference data for two Li-based half-Heusler compounds that have received little attention in literature, particularly LiTiB. By establishing clear structure–property relationships and highlighting the influence of atomic configuration and p–d hybridization on both mechanical and electronic behavior, the present results offer a solid foundation for future theoretical studies and may encourage experimental investigations of Li-based half-Heusler systems.

It should be noted that the present study is restricted to zero-temperature calculations within the GGA framework; therefore, finite-temperature effects, lattice vibrations, or electronic correlation beyond standard DFT. Moreover, while the metallic nature and mechanical stability of these compounds are clearly established, no direct technological applications are claimed at this stage.

Data Availability:

All data supporting the findings of this study are available upon request.

Acknowledgments

I would like to thank the Computational Materials Physics Group for providing access to the WIEN2k software and computing facilities used in this study.

References

Al Rahal Al Orabi, Rabih Boucher, Benoît Fontaine, Bruno Gall, Philippe Candolfi, Christophe Lenoir, Bertrand Gougeon, Patrick Halet and Jean-François. "Towards the prediction of the transport properties of cluster-based molybdenum chalcogenides†." Journal of Materials Chemistry C 5 (2017): 46. https://doi.org/10.1039/C7TC03977H.

Blaha, P., K. Schwarz, F. Tran, R. Laskowski, G. K. H. Madsen, and L. D. Marks. "WIEN2k: An APW+lo Program for Calculating the Properties of Solids." Journal of Chemical Physics 152 (2020): 074101. https://doi.org/10.1063/1.5143061.

Blaha, P., K. Schwarz, G. K. H. Madsen, D. Kvasnicka, and J. Luitz. WIEN2k: An Augmented Plane Wave Plus Local Orbitals Program for Calculating Crystal Properties. Vienna: Technische Universität Wien, 2001. https://openalex.org/10.1063/W77753788.

Chadov, S., X. Qi, J. Kübler, G. H. Fecher, C. Felser, and S. C. Zhang. "Tunable Multifunctional Topological Insulators in Ternary Heusler Compounds." Nature Materials 9 (2010): 541–545. https://doi.org/10.1038/nmat2770.

De Groot, R. A., F. M. Mueller, P. G. van Engen, and K. H. J. Buschow. "New Class of Materials: Half-Metallic Ferromagnets." Physical Review Letters 50 (1983): 2024–2027. https://doi.org/10.1103/PhysRevLett.50.2024.

Felser, C., G. H. Fecher, and B. Balke. "Spintronics: A Challenge for Materials Science and Solid-State Chemistry." Angewandte Chemie International Edition 46 (2007): 668–699. https://doi.org/10.1002/anie.200601815.

Galanakis, I., P. H. Dederichs, and N. Papanikolaou. "Slater–Pauling Behavior and Origin of the Half-Heusler Alloys." Physical Review B 66 (2002): 174429. https://doi.org/10.1103/PhysRevB.66.174429.

Graf, T., C. Felser, and S. S. P. Parkin. "Simple Rules for the Understanding of Heusler Compounds." Progress in Solid State Chemistry 39 (2011): 1–50. https://doi.org/10.1016/j.progsolidstchem.2011.02.001.

Hill, R. "The Elastic Behaviour of a Crystalline Aggregate." Proceedings of the Physical Society. Section A 65 (1952): 349–354. https://doi.org/10.1088/0370-1298/65/5/307.

Hohenberg, P., and W. Kohn. "Inhomogeneous Electron Gas." Physical Review 136 (1964): B864–B871. https://doi.org/10.1103/PhysRev.136.B864.

Kohn, W., and L. J. Sham. "Self-Consistent Equations Including Exchange and Correlation Effects." Physical Review 140 (1965): A1133–A1138. https://doi.org/10.1103/PhysRev.140.A1133.

Lee, J. H., H. S. Kim, W. S. Kim, and J. H. Shim. "Electronic Structure and Thermoelectric Properties of Sb-Based Semiconducting Half-Heusler Compounds." Physical Review B 83 (2011): 085204. https://doi.org/10.1103/PhysRevB.83.085204.

Marder, M. P. Condensed Matter Physics. 2nd ed. New York: Wiley, 2010. https://doi.org/10.1002/9780470949955.

Methfessel, M., and A. T. Paxton. "High-Precision Sampling for Brillouin-Zone Integration in Metals." Physical Review B 40 (1989): 3616–3621. https://doi.org/10.1103/PhysRevB.40.3616.

Mogulkoc, Y., and Y. O. Ciftci. "Investigation on Structural, Elastic, Electronic and Vibrational Properties of LiTiAl Half-Heusler Compound Using First-Principles Methods." Crystal Structure Theory and Applications 6 (2017): 38–46. https://doi.org/10.17776/cumuscij.296598.

Mouhat, F., and F.-X. Coudert. "Necessary and Sufficient Elastic Stability Conditions in Various Crystal Systems." Physical Review B 90 (2014): 224104. https://doi.org/10.1103/PhysRevB.90.224104.

Murnaghan, F. D. "The Compressibility of Media Under Extreme Pressures." Proceedings of the National Academy of Sciences of the United States of America 30 (1944): 244–247. https://doi.org/10.1073/pnas.30.9.244.

Nashia, T.S., Mim, M.H., Tarekuzzaman, M. et al. Computational investigation of LiMgZ half-heusler phases where Z = P, as, and Bi for optoelectronic and photoelectronic applications. Scientific reports 15, 33943 (2025). https://doi.org/10.1038/s41598-025-10593-y

Perdew, J. P., K. Burke, and M. Ernzerhof. "Generalized Gradient Approximation Made Simple." Physical Review Letters 77 (1996): 3865–3868. https://doi.org/10.1103/PhysRevLett.77.3865.

Pugh, S. F. "Relations Between the Elastic Moduli and the Plastic Properties of Polycrystalline Pure Metals." Philosophical Magazine 45 (1954): 823–843. https://doi.org/10.1080/14786440808520496.

Singh, D. J., and L. Nordström. Planewaves, Pseudopotentials and the LAPW Method. Berlin: Springer, 2006. https://doi.org/10.1007/978-0-387-29684-5_5.

Tobola, J., and J. Pierre. "Electronic Phase Diagram of the XTZ (X = Fe, Co, Ni; T = Ti, Zr, Hf; Z = Al, Ga, In, Sn) Half-Heusler Compounds." Journal of Alloys and Compounds 296 (2000): 243–252. https://doi.org/10.1016/S0925-8388(99)00549-6.

Wang,Y.S., R.K. Linghu, W. Zhang, Y.C. Shao, A.D. Lan, and J. Xu. "Study on deformation behavior in supercooled liquid region of a Ti-based metallic glassy matrix composite by artificial neural network." Journal of Alloys and Compounds 844 (2020): 155761. https://doi.org/10.1016/j.jallcom.2020.155761.